metals

MDPI

Article

Effect of Flux Ratio on Droplet Transfer Behavior in Metal-Cored Arc Welding

Ngoc Quang Trinh [1,2], Shinichi Tashiro [1,*], Tetsuo Suga [1], Tomonori Kakizaki [3], Kei Yamazaki [3], Tomokazu Morimoto [3], Hiroyuki Shimizu [3], Ackadech Lersvanichkool [4], Hanh Van Bui [2] and Manabu Tanaka [1]

[1] Joining and Welding Research Institute, Osaka University, Osaka 567-0047, Japan; n.trinh@jwri.osaka-u.ac.jp (N.Q.T.); suga@jwri.osaka-u.ac.jp (T.S.); tanaka@jwri.osaka-u.ac.jp (M.T.)
[2] School of Mechanical Engineering, Hanoi University of Science and Technology, Hanoi 100-000, Vietnam; hanh.buivan@hust.edu.vn
[3] Kobe Steel, Ltd., Fujisawa 251-8551, Japan; kakizaki.tomonori@kobelco.com (T.K.); yamazaki.kei@kobelco.com (K.Y.); morimoto.tomokazu@kobelco.com (T.M.); shimizu.hiroyuki@kobelco.com (H.S.)
[4] Thai Kobelco Welding Co., Ltd., Muang 10280, Thailand; ackadech.lers@kobelco.com
* Correspondence: tashiro@jwri.osaka-u.ac.jp; Tel.: +81-6-6879-8666

Abstract: The effect of flux ratio on metal transfer behavior during metal-cored arc welding was elucidated through investigation using a standard solid wire and three metal-cored wires with flux mass ratios of **(2-2)** 10%, 15%, and 20%. Investigation was performed using a shadowgraph technique based on images recorded with a high-speed camera equipped with back-laser illumination. We observed that the droplet transfer frequency increased with both the welding current and flux ratio, with the effect of flux ratio being more dominant at low currents. We surmise that this is because the wire sheath area decreases as the flux ratio is increased. Hence, when the welding current is the same, a reduction in the sheath area (i.e., an increase in flux content) leads to an increase in the current density in the sheath, which enlarges the electromagnetic force at the tip of the wire and aids droplet detachment. Conversely, Joule heating is higher at high welding currents than at low currents. This increased temperature shortens the flux column inside the wire, such that the current flow into the molten droplets is more uniform. Hence, the droplet transfer frequency does not increase significantly if the flux ratio is increased in the high current range.

Keywords: metal-cored arc welding; metal-cored wire; flux ratio; droplet transfer; current path

check for updates

Citation: Trinh, N.Q.; Tashiro, S.; Suga, T.; Kakizaki, T.; Yamazaki, K.; Morimoto, T.; Shimizu, H.; Lersvanichkool, A.; Bui, H.V.; Tanaka, M. Effect of Flux Ratio on Droplet Transfer Behavior in Metal-Cored Arc Welding. *Metals* **2022**, *12*, 1069. https://doi.org/10.3390/met12071069

Academic Editor: Xiangdong Gao

Received: 10 May 2022
Accepted: 18 June 2022
Published: 22 June 2022

Publisher's Note: MDPI stays neutral with regard to jurisdictional claims in published maps and institutional affiliations.

Copyright: © 2022 by the authors. Licensee MDPI, Basel, Switzerland. This article is an open access article distributed under the terms and conditions of the Creative Commons Attribution (CC BY) license (https://creativecommons.org/licenses/by/4.0/).

1. Introduction

At present, gas metal arc welding (GMAW) is the most widely used welding process in the manufacturing and construction industries [1]. With this process, the stability of the arc needs to be controlled to obtain a weld of the desired quality, as the transfer of molten metal from the electrode to the weld pool determines the integrity of the weld [1–3]. A range of parameters in the welding process can cause variations in metal transfer, leading to short-circuit, globular, and spray transfer modes [3,4], that affect weld quality.

An important improvement to GMAW is the flux-cored arc welding (FCAW) process, in which a tubular wire filled with a powder flux and coated with a metal sheath is used to facilitate joining between a wider range of materials. Here, welding wires can be classified into slag systems, such as metal, rutile, and basic flux-cored wires [5], according to the main constituent of the internal flux. As well as increasing the applicability of FCAW welding, the addition of flux components makes metal transfer more complex, as a wider range of parameters can be controlled during processing [6,7]. For example, Liao and Chen [8] observed that flux-cored wires produce a reduced amount of spatter compared to solid wires, regardless of the composition of the shielding gas. Bauné et al. [9] developed experimental flux-cored wires with modified flux compositions to improve arc stability

and welding performance. Srinivasan et al. [10] observed that performing FCAW in surface tension transfer mode reduced the fume emission rate (FER) by up to 50% **(2-4)**.

Numerous further studies have demonstrated that metal transfer in FCAW is affected by the composition of the flux as well as the structure of the wire electrode. For instance, following thermodynamic calculations, Matsushita and Liu [11] demonstrated that the addition of fluorides is effective in controlling the hydrogen content in a steel weld metal, and thus reducing the risk of cold cracking. Potassium fluoride was particularly effective in reducing the diffusible hydrogen in the weld metal. Similarly, comparisons of the effect of a range of fluorides on FCAW indicated that although more vaporizable fluorides are more effective in reducing the hydrogen content of a weld, they also result in an unstable arc [12,13]. From their study of hydrogen trapping with yttrium, Lensing et al. [14] reported that the spray transfer mode promotes a more efficient transfer of yttrium to the weld deposit than the globular transfer mode, resulting in reduced amounts of diffusible hydrogen. Valensi et al. [15] reported that when using an Ar-CO_2 shielding gas with a CO_2 content of up to 60 vol% at 330 A, the presence of alkaline elements stabilizes the spray arc. Trinh et al. [16] observed that the addition of only a small amount of sodium can significantly increase the metal transfer frequency by reducing the arc pressure and enhancing the electromagnetic force acting on the neck of the molten droplet at the wire tip.

Despite the range of studies focusing on flux composition, the impact of the wire electrode structure on metal transfer has rarely been analyzed. Studies such as Matsuda et al.'s [17] investigation of the effect of the geometrical characteristics of the wire cross-section on metal transfer have focused on electrode structure. This study highlighted that in free-flight mode, large droplets are formed at the sides of the tips of hollow-sheathed wires, while the droplets formed with folded-sheath wires are smaller than the wire diameter. In contrast, Suga and Kobayashi [18] reported that, with rutile flux-core wires, the cross-sectional shape of a wire has almost no effect on droplet transfer, and that the flux content of the wire is the most important parameter for controlling droplet transfer. Furthermore, the presence or absence of seams on a wire electrode also contributes to the amount of diffusible hydrogen in a weld bead [19]. For instance, the effectiveness of Mukai et al.'s [20] novel welding torch for reducing diffusible hydrogen was strongly affected by the use of a seamed flux-cored wire. Ushio et al. [21] observed that the effect of Ohmic heating and arc heating on the melting rate of flux-cored wire is reduced compared to the effect on the melting rate of solid wires. Yamamoto et al. [22] observed that at low currents (<150 A), both the FER and the heat content of droplets increased with the flux ratio of a rutile flux-cored wire. These studies demonstrate that wire structure is a key factor in determining welding arc stability, especially when metal-cored wires, whose main core composition is iron powder, are used. However, the mechanism underlying the influence of the flux ratio on metal-cored wires is not yet well understood.

In this study, we examined the effects of flux ratio on the metal transfer behavior of metal-cored wires. A solid wire without flux content and three prototype electrodes with different flux mass ratios were investigated as part of a parametric study. The metal transfer behavior of the metal-cored wires was characterized using the shadowgraph technique, based on images obtained from a high-speed camera to clarify the influence of flux ratio.

2. Experimental Method

2.1. Common Welding Conditions

The investigation of metal-cored arc welding conducted in this study focused on a bead-on-plate process. Here, 300 mm × 50 mm × 9 mm mild steel plates (SS400—JIS G 3101) were used as the base metal. We characterized the effect of flux ratio on metal transfer using four wires with a diameter of 1.2 mm. The first wire (Wire 1) was a commercially available solid wire (JIS Z3312 YGW11) with an AWS classification of A5.18 ER70S-G and a metal flux of **(2-8)** 0%, while Wires 2, 3, and 4 were prototype metal-cored wires with an AWS classification corresponding to A5.20 E70T-1C. The flux mass ratios of the latter three wires were 10%, 15%, and 20%, respectively. In addition, the total wire area of Wires 1, 2, 3,

and 4 were 1.13 mm^2, 1.10 mm^2, 1.12 mm^2, and 1.10 mm^2; meanwhile, the sheath areas of the three metal-cored wires were 0.93 mm^2, 0.87 mm^2, and 0.80 mm^2, respectively. **(2-10)** Cross-sections of the three metal-cored wires are presented in Figure 1. Summaries of the chemical compositions of all the wires are listed in Table 1.

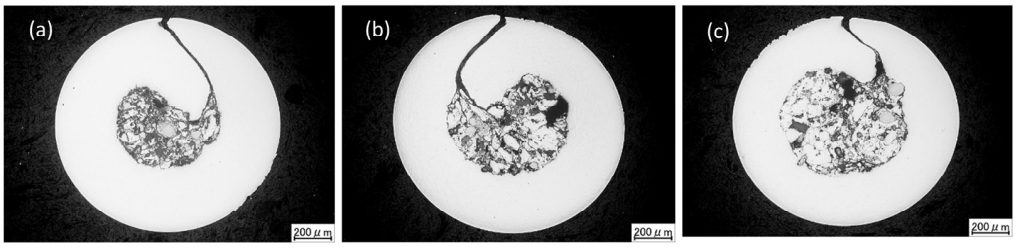


Figure 1. Cross-section of Wire 2 (**a**), Wire 3 (**b**), and Wire 4 (**c**).

Table 1. Chemical composition (mass%) of wires investigated in this study.

Wire	C	Si	Mn	Cu	Al	Ti + Zr	SiO_2	TiO_2
Wire 1	0.04	0.73	1.58	0.23	-	0.22	-	-
Wire 2	0.04	0.90	2.00	-	0.26	-	0.23	0.33
Wire 3	0.04	0.90	2.00	-	0.26	-	0.23	0.33
Wire 4	0.04	0.90	2.00	-	0.26	-	0.23	0.33

Welding was conducted in DCEP mode using a DP-350 welding machine (OTC Daihen, Kobe, Japan) connected to a wire-feeding system. Experiments were conducted at 220 A, 250 A, and 280 A, which correspond to low current, medium current, and high current ranges, respectively. The welding voltage was adjusted from 28.5 V to 33.0 V to maintain the arc length constant at approximately 3.2 mm. An **(2-12)** Ar + 20% CO_2 shielding gas was used in welding, with the flow rate controlled at 20 l/mm. The welding torch was fixed above the base metal to maintain a contact tip to work distance of 20 mm. The welding travel speed was maintained at 5 mm/s using an actuator.

2.2. Observation of Metal Transfer

Metal transfer behavior during welding was observed using a shadowgraph technique. The experimental setup for these observations consisted of a laser-assisted high-speed camera system [23]. To ensure clear visualization of individual droplets, the high-speed camera (Memrecam Q1v, Nac Image Technology, Minato, Japan) in this setup was equipped with an objective lens (AF Micro-NIKKOR, Nikon, Minato, Japan) with a focal length of 200 mm, a focus ratio of 1/4, and an aperture value of f/5.6. Videos were recorded at a frame rate of 4000 fps, with an exposure time of 20 μs. The resolution of each frame in a video was 640 pixels × 480 pixels. Molten droplets were illuminated from the opposite side of the camera using a pulsed laser beam with a wavelength of 640 nm generated by the Cavilux HF laser system (Cavitar, Tampere, Finland). The laser beam was aligned to the optical axis of the camera and perpendicular to the arc and welding direction, to enable the camera to capture shadowgraph images of the wire and molten droplet. Five neutral-density filters (ND8) were placed in front of the camera to ensure the images were not saturated with illumination from the arc light and the laser. An illustration of the experimental setup is shown in Figure 2.

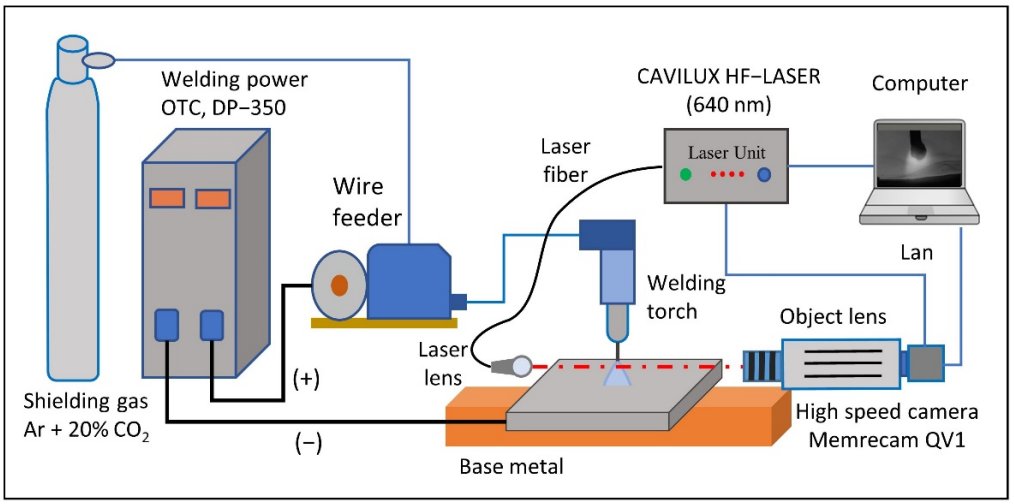


Figure 2. Schematic illustration of metal transfer observation experiment.

3. Results and Discussions

3.1. Metal Transfer Behavior

Sequential images of the typical metal droplet transfer behavior of all four wires are shown in Figure 3. This figure considers the effect of the flux ratio of the wire on transfer behavior in the medium current range. Figure 3a presents the transfer cycle of Wire 1, which has no flux content. Here, a molten droplet was detached from the wire at 0 ms. Another droplet that gradually increased in size was subsequently formed at 6.5 ms. During the growth period (from 9.75 ms to 26 ms), **(2-13)** this droplet was pushed upward by the combination of pressure from the arc and repulsive force due to the metal evaporation of the droplet. In this case, the arc was concentrated at the bottom of the droplet, which hindered droplet detachment. The droplet was repelled backward following detachment at 29.75 ms. These characteristics indicate repelled globular mode metal transfer. In contrast, the spray drop transfer mode was observed in the three metal-cored wires with added flux. Figure 3b shows that with Wire 2, transfer was completed after 6.25 ms. Following detachment of the initial droplet at 0 ms, the subsequent droplet expanded between 1 ms and 6 ms, and its surface was distorted rapidly. Figure 3c indicates that this droplet formation process was completed within 4.5 ms (from 0.75 ms to 5.25 ms) in Wire 3. Similarly, when the flux mass ratio was increased to 20% (Wire 4), the droplet transfer cycle was completed after 4.75 ms, as shown in Figure 3d. Finally, with all three metal-cored wires, the droplet diameter was observed to be almost equal to the wire diameter.

Figure 4 depicts droplet transfer from Wire 3 in the three different current ranges, for illustration of the effect of welding current on metal transfer behavior. Figure 4a shows the transfer cycle at a welding current of 220 A, where the droplet was generated and detached from the wire between 1.25 ms and 10.25 ms. Figure 4b depicts the medium current range considered in Figure 3 and is thus identical to Figure 3c. Hence, increasing the welding current from 220 A to 250 A decreased the time for a droplet to transfer from the wire tip to the weld pool from 10.25 ms to 5.25 ms. Figure 4c shows that increasing this current to 280 A decreased the duration of droplet transfer even further, such that the transfer cycle was completed after only 4.5 ms. Here, a long taper can be observed in the molten metal at the tip of the wire. As the arc was attached to this taper, the arc covered the entire droplet when it was generated at 1.5 ms, and during its subsequent expansion, until complete detachment at 4.5 ms. This wire thus exhibited globular transfer in the low current range, and spray transfer in the medium and high current ranges.

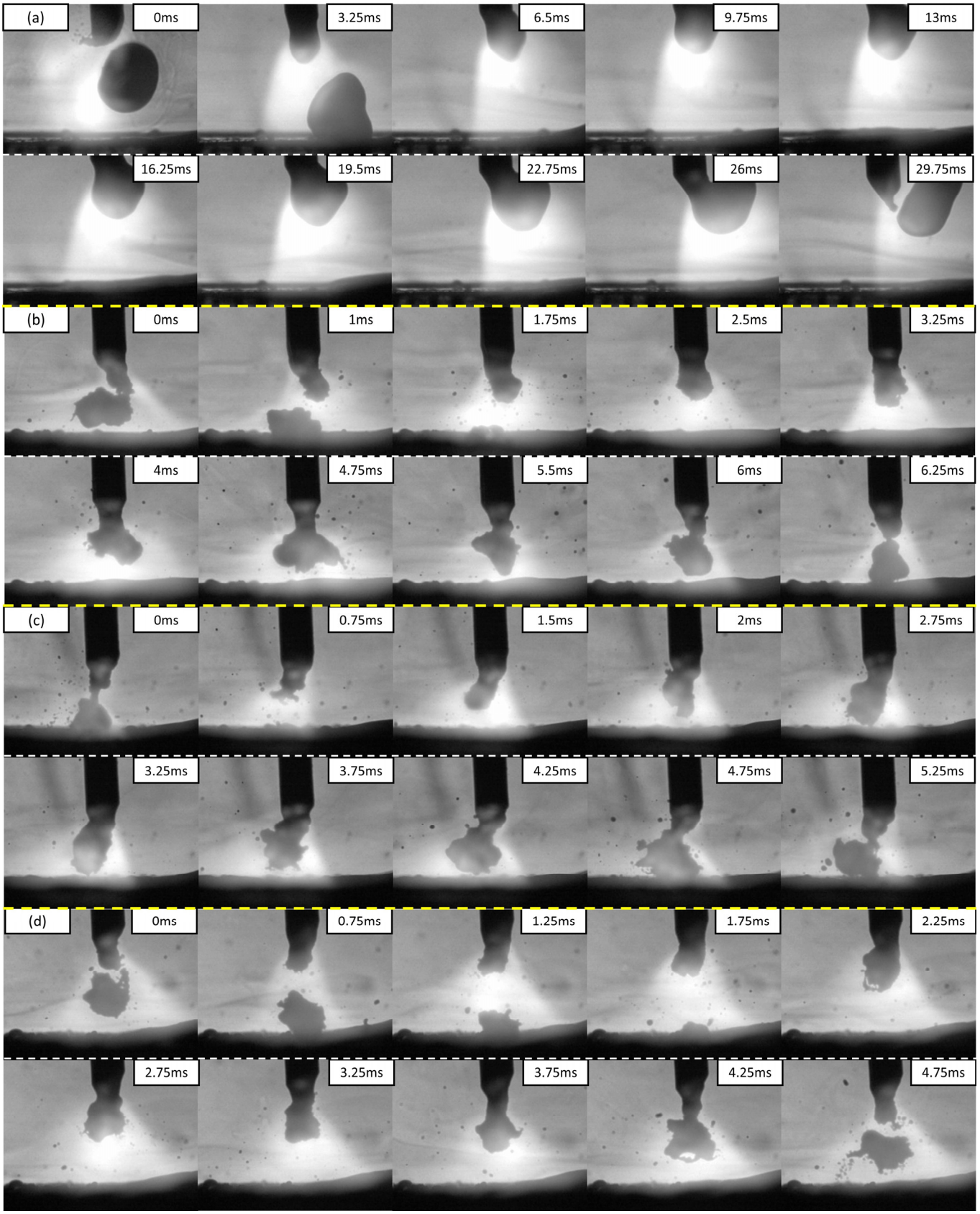


Figure 3. Sequential images of droplet transfer in the medium current range for (**a**) Wire 1, (**b**) Wire 2, (**c**) Wire 3, and (**d**) Wire 4.

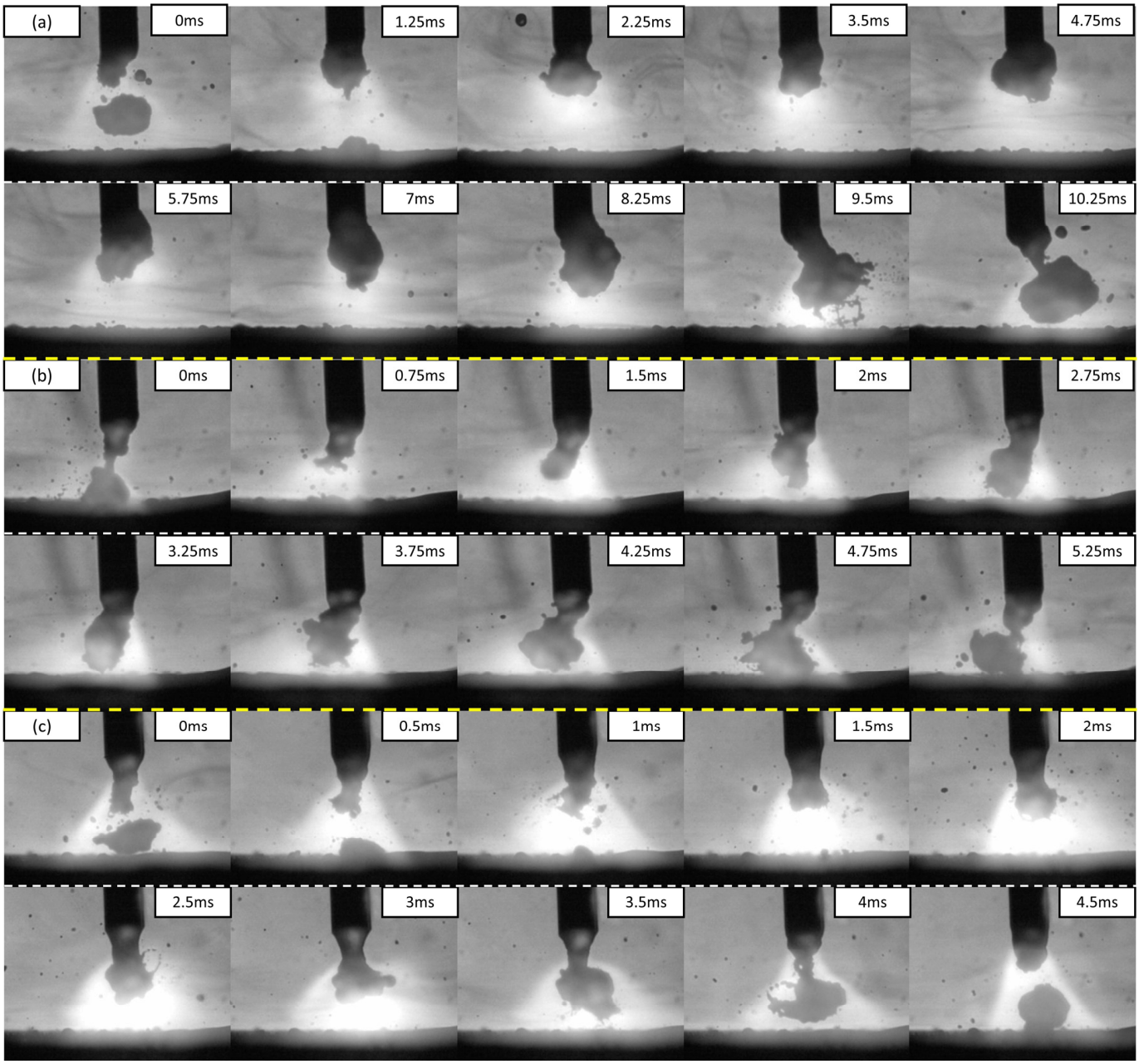
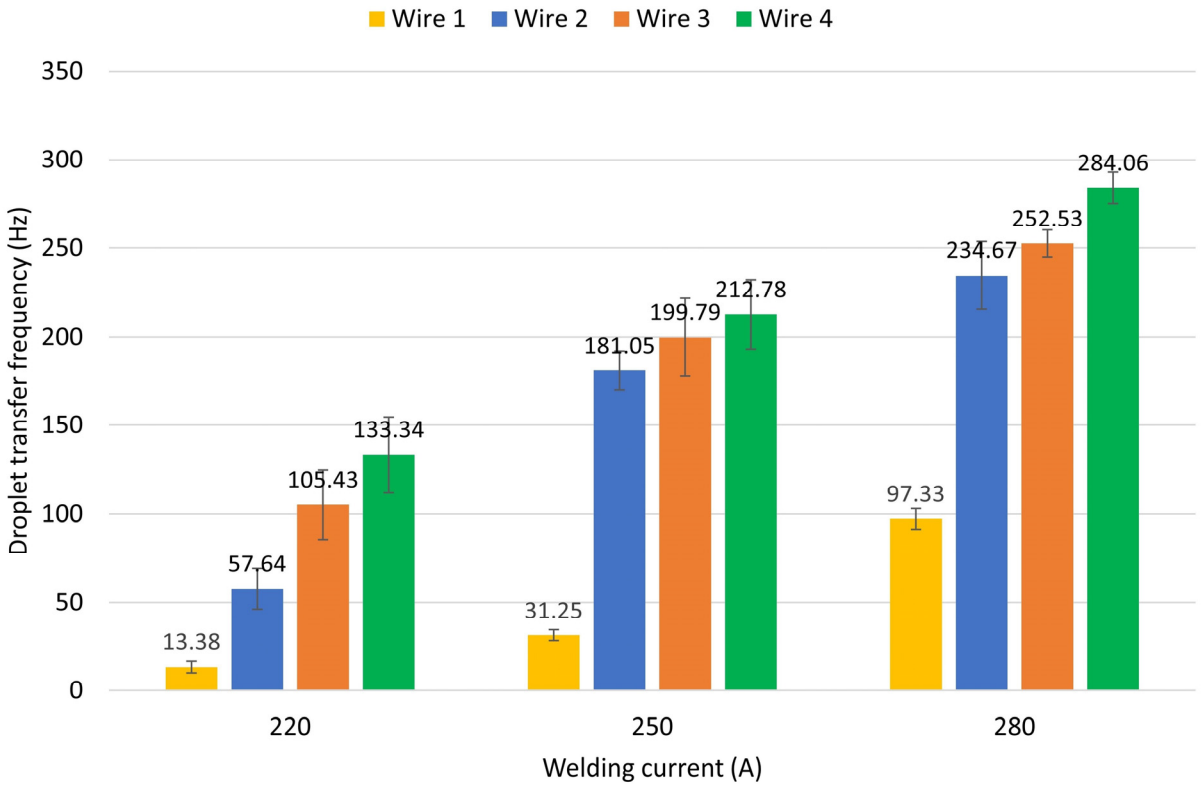


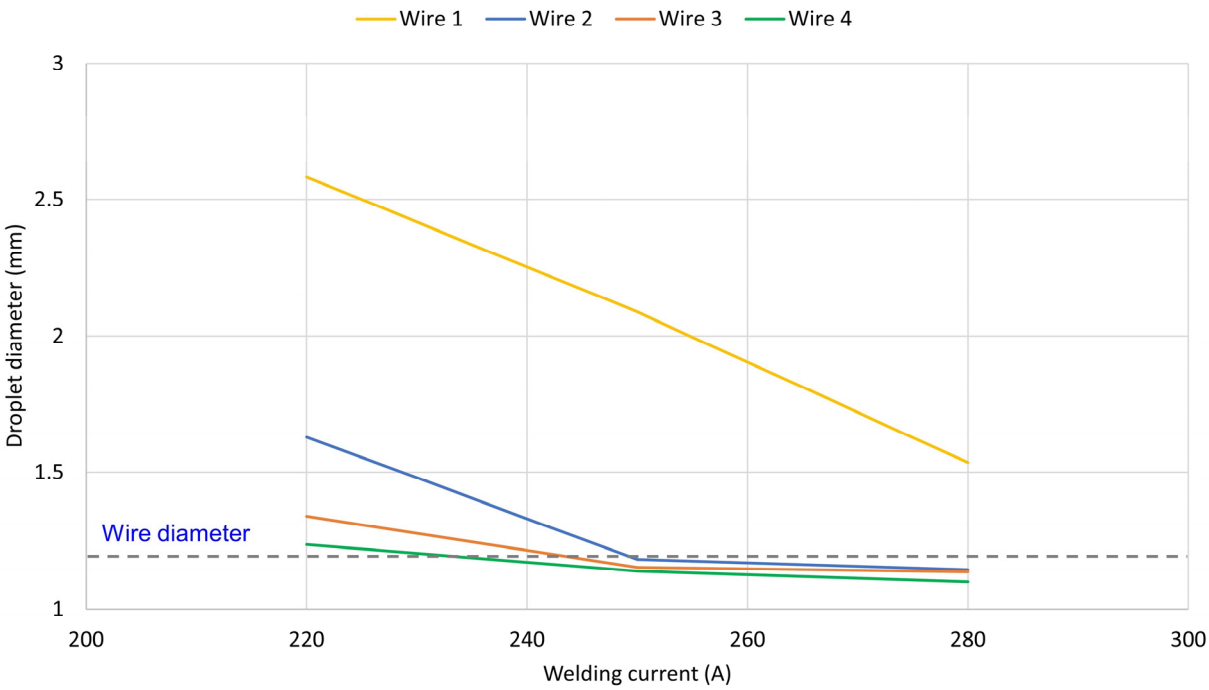
Figure 4. Metal transfer behavior of Wire 3 in the (**a**) low current range, (**b**) medium current range, and (**c**) high current range.

Figure 5a shows the metal transfer frequencies of all four wires. The values in this graph are the average frequency from five measurements, while the error bars indicate the standard deviation. Here, it can be seen that the droplet transfer frequency increases with both the flux ratio and the welding current. In the low welding current range (220 A), the minimum transfer frequency of Wire 1 was 13.38 Hz. This frequency increased to 57.64 Hz, 105.43 Hz, and 133.34 Hz for Wires 2, 3, and 4, which have flux mass ratios of 10%, 15%, 20%, respectively. In the medium current range (250 A), the transfer frequency of Wire 1 (31.25 Hz) was much lower than those of Wires 2, 3, and 4 (181.05 Hz, 199.79 Hz, and 212.78 Hz, respectively). Although the transfer frequency of Wire 1 increased significantly (to 97.33 Hz) in the high current range, the transfer frequencies of Wires 2, 3, and 4 (234.67 Hz, 252.53 Hz, and 284.06 Hz, respectively) did not increase accordingly. These

results indicate that the effect of flux ratio on droplet transfer frequency is most significant in the low current range.



(**a**)



(**b**)

Figure 5. Variation of (**a**) metal transfer frequency and (**b**) droplet diameter with welding current.

Figure 5b shows the diameter of the molten metal droplets produced by all the wires, calculated based on the melting velocity and the transfer frequencies shown in Figure 5a. This figure indicates that Wire 1 exhibited globular transfer in all welding conditions. In contrast, globular transfer was only observed with the metal-cored wires at the low welding current (220 A); spray transfer was observed at medium and high currents. The image thus indicates that the droplet diameter decreases when the welding current increased or the flux ratio is increased.

3.2. Effect of Flux Ratio and Welding Current

A schematic of the four wires at 250 A is presented in Figure 6 for explanation of the influence of the flux ratio on metal transfer behavior. The current flow inside Wire 1 is thought to be uniform, as shown in Figure 6a. Conversely, in the metal flux-cored wires, due to the low electrical conductivity of the flux [24], current flow is concentrated to the metal sheath of the wire, as shown in Figure 6b–d. Hence, the current density is higher in these wires than that in the solid wire.

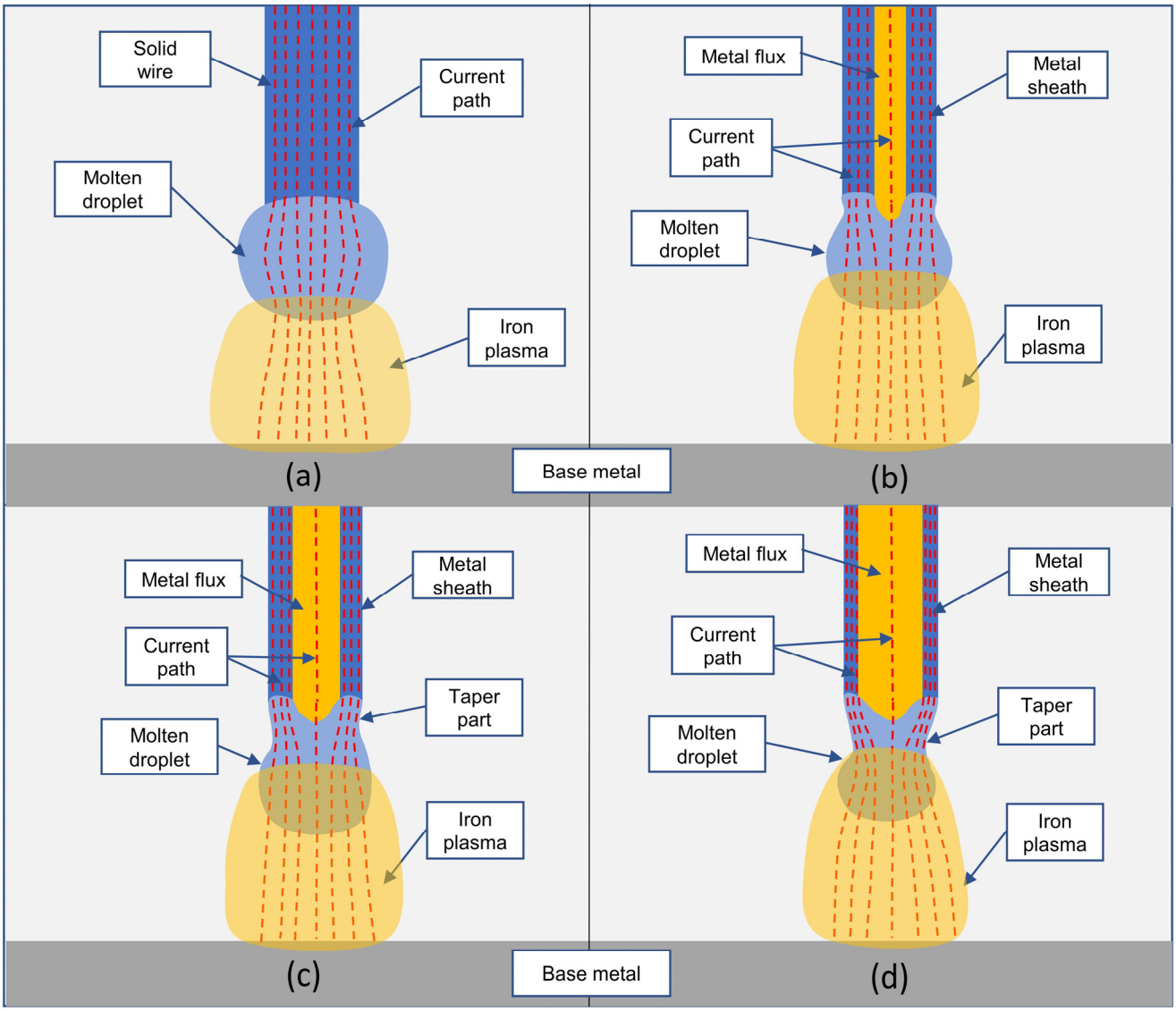


Figure 6. Schematic of metal transfer behavior in (**a**) Wire 1, (**b**) Wire 2, (**c**) Wire 3, and (**d**) Wire 4 at 250 A.

In Figure 6a, the arc attached to the bottom of the droplet consisted primarily of iron plasma, leading to a high arc pressure that prevents droplet detachment. The position of the arc attached to the bottom of the metal droplet was higher in Figure 6b than in Figure 6a. However, no molten metal taper was observed before droplet detachment in either of the scenarios these schematics represent, as shown in Figure 3a at 26 ms, and Figure 3b at 6 ms. In contrast, a taper appeared in the molten metal at the tip of the electrode in the scenarios represented by Figure 6c,d, as demonstrated by Figure 3c at 4.75 ms and Figure 3d at 4.25 ms. In these two cases, the arc climbed up and covered a larger part of the droplet. This phenomenon can be explained as follows.

Increasing the flux ratio leads to decreasing the sheath area of the wires and, therefore, raising the current density in the cross-sectional area of the metal sheath while maintaining the same welding current. The increased current density thus promotes the electromagnetic force acting at the neck of the molten droplet, which leads to the Pinch effect becoming more effective in gradually decreasing the diameter of the molten metal at the tip of the wire to form the taper part [25,26]. **(1-4)** The electromagnetic force (Lorentz force) can be, respectively, calculated as follows:

$$\vec{F_{em}} = \vec{j} \times \vec{B}$$

where $\vec{F_{em}}$ is the electromagnetic force (N/m^3), $\vec{j}$ is the current density (A/m^2), and $\vec{B}$ is the magnetic flux density (N/A·m).

The current density of the wire can be calculated as follows:

$$j = \frac{I}{S}$$

where I is the current in the wire (A), and S is the conductive cross-section of the wire (m^2). Meanwhile, the magnetic flux density B in circles around the wire at a distance r from the wire can be calculated as follows:

$$B = \frac{\mu_0 I}{2\pi r}$$

where μ_0 is the permeability of free space, $\mu_0 = 4\pi \times 10^{-7}$ (N/A^2).

The Lorentz force acting on the wires is now compared. The forces were assumed to act on the interface of the solid part and liquid part on the wire surface. For simple calculation, the low welding current was used because of the unmelted flux at the neck position of the droplet. In the case of medium and high welding current, the conductive cross-section area may vary depending on the position of melting flux. The calculated forces of Wire 1, Wire 2, Wire 3, and Wire 4 are 14.28×10^6 N/m^3, 17.35×10^6 N/m^3, 18.54×10^6 N/m^3, and 20.17×10^6 N/m^3, respectively. It is obvious that the electromagnetic force acting on the wire electrode increased when the flux ratio increased. When the taper part appeared, the arc expanded upward to attach at a higher position and cover a larger part of the droplet; consequently, increasing the droplet transfer frequency.

Figure 7 presents a schematic explanation of the effect of welding current on the metal transfer behavior of a metal flux-cored wire with a flux ratio of 15%. Figure 7a shows that at low currents, the arc is concentrated at the bottom of the droplet. Here, we assume that the flux column inside the wire occupies a significant portion of the droplet. Furthermore, the current intensity at the neck of the droplet was not high enough to induce rapid detachment. An actual image of this scenario is presented in Figure 4a at 9.5 ms. Figure 7b explores the scenario when the current was 250 A. Here, the arc moves upward and attaches to the droplet at a higher position. Thus, the molten metal tapers slightly at the tip of the wire, as observed in Figure 4b at 4.25 ms. Finally, at 280 A, the arc completely covers the droplet, as shown in Figure 7c. In this case, the taper in the molten droplet is sharper, as demonstrated in Figure 4c at 3.5 ms.

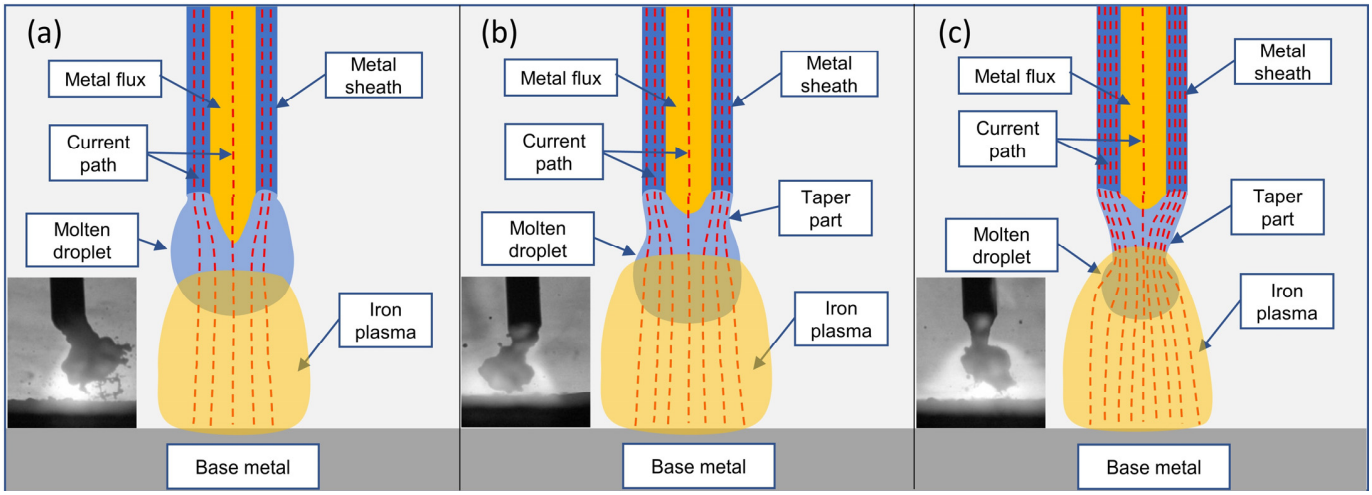


Figure 7. Schematic of metal transfer behavior in Wire 3 at (**a**) 220 A, (**b**) 250 A, and (**c**) 280 A. **(1-4) (2-16)**.

The reason why the effect of flux ratio on droplet transfer frequency is significant in low current range is considered to be related to the state of the unmelted flux column. Most of the current can be assumed to conduct in the sheath and molten droplet due to the low electrical conductivity of unmelted flux. The temperature in those regions is increased by the Joule heating effect, causing thermal conduction to the unmelted flux. This Joule heating effect is larger at high currents than that at low currents. Hence, at high currents, the flux column is shortened by melting. As unmelted flux in the droplet prevents current flow, the shortening of the flux column makes the current flow in the molten droplet more uniform. The contribution of Joule heating explains the diminishing effect of increased flux ratios on droplet transfer frequency in the high current range.

For verification of the explanations presented by the schematics in Figure 7, we analyzed the cross-section of Wire 3 after welding using scanning electron microscopy (SEM) and energy-dispersive X-ray spectroscopy (EDS) to identify the presence of unmelted metal flux inside the droplet. SEM images of the longitudinal section of wire after welding at 220 A, 250 A, and 280 A are shown in Figure 8a–c. As the flux in the metal-cored wire used in this study includes Al and SiO_2, we focused EDS analysis on identification of aluminum and silicon. The distribution of these elements as revealed by EDS area analysis is shown following the SEM image. From this, we observed that at the low current, unmelted flux could be found in the spherical part of the droplet as in Figure 8a. In contrast, the absence of Al and Si at the tip of the wire in the EDS images shown in Figure 8b,c indicate that no unmelted metal flux remained inside the droplet after welding at medium and high current, respectively. In addition, the distributions of these elements are similar in both figures, implying that the change between the two currents did not affect the wire's droplet transfer behavior significantly. This implication is consistent with the metal transfer frequency results shown in Figure 5a.

(2-1) There are other possible effects on the transfer behavior by chemical effects on the viscosity and surface tension of the molten droplet. Both were discussed by Vanlesi et al. [15] by comparing the influence of wire composition on anode microstructure and metal transfer behavior in GMAW. The results show that surface tension modification by silicon content is not a key parameter for droplet detachment for considered current density. On the other hand, the viscosity may be a determining factor affecting the metal transfer mode. When the alkaline elements were added to the wire, it allowed spray-like transfer in CO_2 dominant shielding gas. Due to the low viscosity of alkaline elements, the hypothesis of material viscosity was supported. In the present study, the composition of metal-cored wires was maintained. When the flux ratio was varied, the amount of chemical

composition injected into a molten droplet may be affected. However, we assumed that the primary factor that affects the metal transfer behavior is the current density of the wire.

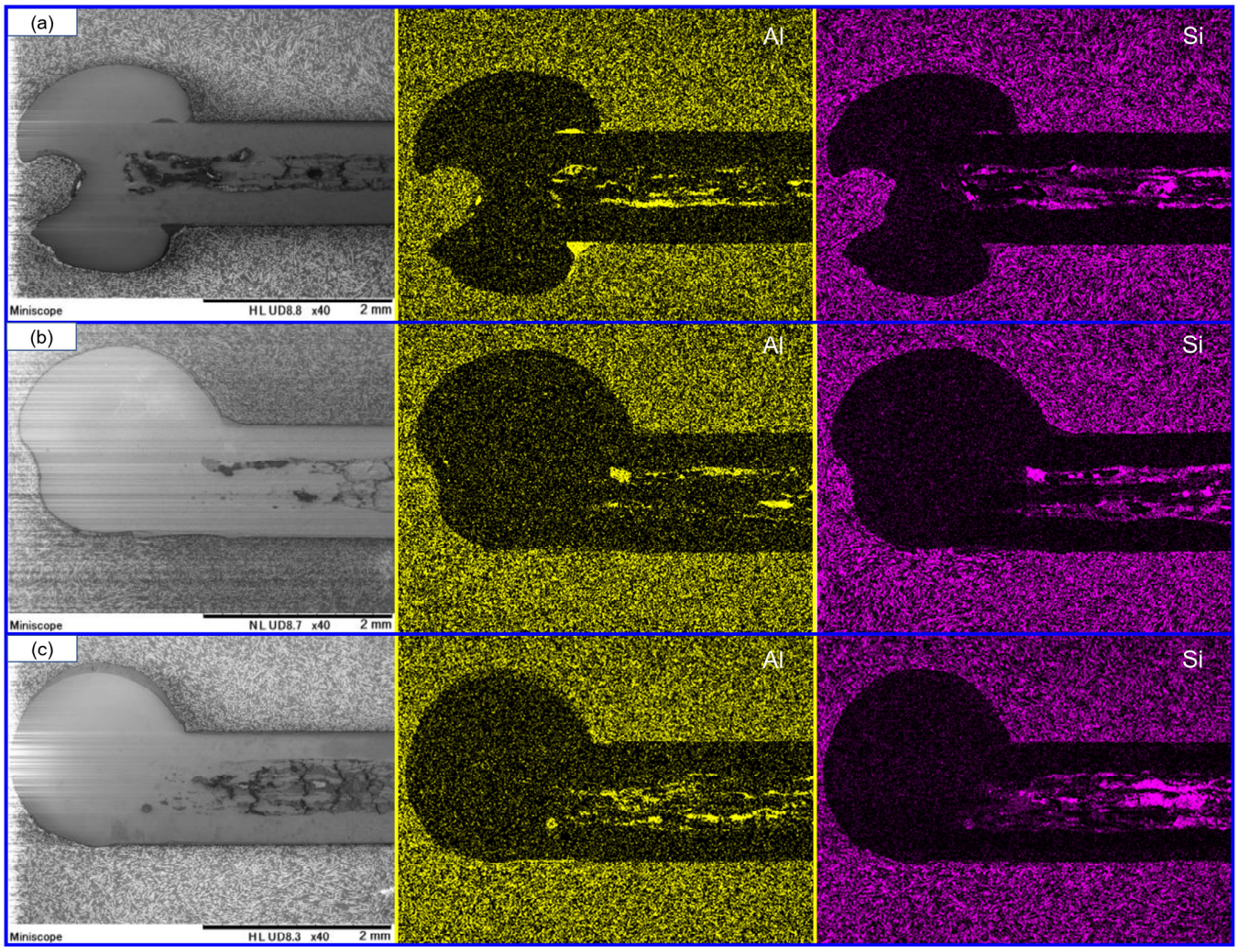


Figure 8. Longitudinal section of Wire 3, distribution of Al, and Si following welding at (**a**) 220 A, (**b**) 250 A, and (**c**) 280 A.

4. Conclusions

In this study, we investigated the mechanism underlying the effects of flux ratio on droplet transfer behavior in metal-cored arc welding, using the shadowgraph technique. Here, we conducted a parametric study based on comparison of a solid wire and three prototype wires with varying flux ratios. Conclusions can be drawn from the results as follows:

1. The metal transfer frequency increased, while the droplet diameter decreased when either the welding current or flux ratio was increased.
2. The sheath area of the wire decreased as the flux ratio was increased. Thus, if the current is the same, a reduction in the metal sheath area increases the current density in the sheath of the wire. Consequently, the electromagnetic force at the tip of the wire increases and enhances droplet detachment.
3. The effect of flux ratio on droplet transfer frequency was more dominant at low currents. This is because Joule heating effects, which shorten the metal flux column, are larger at high welding currents than at low welding currents. This shortened flux column leads to a more uniform current flow into the molten droplets, which counteracts some of the effects obtained by increasing the flux ratio.

A better understanding of the effects of flux ratio on the metal-cored arc welding process can help manufacturers improve their wire designs. Hence, our study can help optimize the performance of this process.

Author Contributions: Conceptualization, methodology, supervision, S.T.; experiment, N.Q.T. and T.K.; writing—original draft preparation, N.Q.T.; writing—review and editing, S.T.; discussion, T.S., K.Y., T.M., H.S., A.L., H.V.B. and M.T. All authors have read and agreed to the published version of the manuscript.

Funding: This research received no external funding.

Institutional Review Board Statement: Not applicable.

Informed Consent Statement: Not applicable.

Data Availability Statement: Data can be available based on the requirements to verify this work.

Acknowledgments: The authors are grateful for the support toward this study by a joint research agreement between the Joining and Welding Research Institute, Osaka University, Japan; Hanoi University of Science and Technology, Vietnam; Kobe Steel Ltd., Japan; Thai Kobelco Welding Co., Ltd., Thailand.

Conflicts of Interest: The authors declare no conflict of interest.

References

1. Kah, P.; Latifi, H.; Suoranta, R.; Martikainen, J.; Pirinen, M. Usability of Arc Types in Industrial Welding. *Int. J. Mech. Mater. Eng.* **2014**, *9*, 1–12. [CrossRef]
2. Fan, H.G.; Kovacevic, R. Droplet Formation, Detachment, and Impingement on the Molten Pool in Gas Metal Arc Welding. *Metall. Mater. Trans. B Process Metall. Mater. Process. Sci.* **1999**, *30*, 791–801. [CrossRef]
3. Hu, J.; Tsai, H.L. Heat and Mass Transfer in Gas Metal Arc Welding. Part II: The Metal. *Int. J. Heat Mass Transf.* **2007**, *50*, 808–820. [CrossRef]
4. Scotti, A.; Ponomarev, V.; Lucas, W. A Scientific Application Oriented Classification for Metal Transfer Modes in GMA Welding. *J. Mater. Process. Technol.* **2012**, *212*, 1406–1413. [CrossRef]
5. Brien, A.O. *Welding Handbook*; American Welding Society Inc.: Miami, FL, USA, 2004; Volume 2, ISBN 0871717298.
6. Starling, C.M.D.; Modenesi, P.J. Metal Transfer Evaluation of Tubular Wires. *Weld. Int.* **2007**, *21*, 412–420. [CrossRef]
7. Wang, W.; Liu, S.; Jones, J. Flux Cored Arc Welding: Arc Signals, Processing and Metal Transfer Characterization. *Weld. J.-Incl. Weld. Res. Suppl.* **1995**, *74*, 369s.
8. Liao, M.T.; Chen, W.J. A Comparison of Gas Metal Arc Welding with Flux-Cored Wires and Solid Wires Using Shielding Gas. *Int. J. Adv. Manuf. Technol.* **1999**, *15*, 49–53. [CrossRef]
9. Bauné, E.; Bonnet, C.; Liu, S. Assessing Metal Transfer Stability and Spatter Severity in Flux Cored Arc Welding. *Sci. Technol. Weld. Join.* **2001**, *6*, 139–148. [CrossRef]
10. Srinivasan, K.; Balasubramanian, V. Effect of Surface Tension Metal Transfer on Fume Formation Rate during Flux-Cored Arc Welding of HSLA Steel. *Int. J. Adv. Manuf. Technol.* **2011**, *56*, 125–134. [CrossRef]
11. Matsushita, M.; Liu, S. Hydrogen Control in Steel Weld Metal by Means of Fluoride Additions in Welding Flux. *Weld. J.* **2000**, *79*, 295-s–303-s.
12. Bang, K.S.; Jung, H.C.; Han, I.W. Comparison of the Effects of Fluorides in Rutile-Type Flux Cored Wire. *Met. Mater. Int.* **2010**, *16*, 489–494. [CrossRef]
13. Kil, W.; Shin, M.; Bang, K. Effects of Fluoride in the Flux on Hydrogen Content in Weld Metal and Operating Behavior in FCAW-S. *J. Weld. Join.* **2017**, *35*, 65–70. [CrossRef]
14. Lensing, C.A.; Park, Y.D.; Maroef, I.S.; Olson, D.L. Yttrium Hydrogen Trapping to Manage Hydrogen in HSLA Steel Welds. *Weld. J.* **2004**, *83*, 254.
15. Valensi, F.; Pellerin, N.; Pellerin, S.; Castillon, Q.; Dzierzega, K.; Briand, F.; Planckaert, J.P. Influence of Wire Initial Composition on Anode Microstructure and on Metal Transfer Mode in GMAW: Noteworthy Role of Alkali Elements. *Plasma Chem. Plasma Process.* **2018**, *38*, 177–205. [CrossRef]
16. Trinh, N.Q.; Tashiro, S.; Tanaka, K.; Suga, T.; Kakizaki, T.; Yamazaki, K.; Morimoto, T.; Shimizu, H.; Lersvanichkool, A. Effects of Alkaline Elements on the Metal Transfer Behavior in Metal Cored Arc Welding. *J. Manuf. Process.* **2021**, *68*, 1448–1457. [CrossRef]
17. Matsuda, F.; Ushio, M.; Tsuji, T.; Mizuta, T. Arc Characteristics and Metal Transfer with Flux-Cored Electrode in CO_2 Shielding (Report I): Effect of Geometrical Shape in Wire Cross-Section on Metal Transfer in Stainless Steel Wire. *Trans. JWRI* **1979**, *8*, 187–192.
18. Suga, T.; Kobayashi, M. Droplet Transfer Phenomena in CO_2 Arc Welding by Flux-Cored Wire. *Q. J. Japan Weld. Soc.* **1985**, *3–2*, 269–276. [CrossRef]

19. Pitrun, M.; Nolan, D.; Dunne, D. Diffusible Hydrogen Content in Rutile Flux-Cored Arc Welds as a Function of the Welding Parameters. *Weld. World* **2004**, *48*, 2–13. [CrossRef]
20. Mukai, N.; Maruyama, T.; Suzuki, R. Research and Development of the Welding Process for Reducing Diffusible Hydrogen. *Q. J. Japan Weld. Soc.* **2018**, *36*, 86–93. [CrossRef]
21. Ushio, M.; Raja, A.; Matsuda, F. Melting Characteristics of Flux Cored Wire. *Trans. JWRI* **1984**, *13*, 1–6.
22. Yamamoto, E.; Yamazaki, K.; Suzuki, K.; Koshiishi, F. Effect of Flux Ratio in Flux-Cored Wire on Wire Melting Behaviour and Fume Emission Rate. *Weld. World* **2010**, *54*, 154–159. [CrossRef]
23. Mamat, S.B.; Tashiro, S.; Tanaka, M.; Yusoff, M. Study on Factors Affecting the Droplet Temperature in Plasma MIG Welding Process. *J. Phys. D. Appl. Phys.* **2018**, *51*, aab128. [CrossRef]
24. Lancaster, J.F. *The Physics of Welding*; Pergamon Press Ltd.: Oxford, UK, 1984; ISBN 0080340768.
25. Hertel, M.; Spille-Kohoff, A.; Füssel, U.; Schnick, M. Numerical Simulation of Droplet Detachment in Pulsed Gas-Metal Arc Welding Including the Influence of Metal Vapour. *J. Phys. D. Appl. Phys.* **2013**, *46*, 224003. [CrossRef]
26. Hertel, M.; Rose, S.; Füssel, U. Numerical Simulation of Arc and Droplet Transfer in Pulsed GMAW of Mild Steel in Argon. *Weld. World* **2016**, *60*, 1055–1061. [CrossRef]